Journal of Luminescence 131 (2011) 25–29

Contents lists available at ScienceDirect

Journal of Luminescence

journal homepage: www.elsevier.com/locate/jlumin

Luminescent and morphological study of Sr_2CeO_4 blue phosphor prepared from oxalate precursors

Jefferson L. Ferrari [a,c,*], Ana M. Pires [b], Osvaldo A. Serra [c], Marian R. Davolos [a]

[a] Instituto de Química, Unesp Univ Estadual Paulista, P.O. Box 355, 14800-970 Araraquara, SP, Brazil
[b] Depto. de Física, Química e Biologia, Faculdade Ciências e Tecnologia, Unesp Univ Estadual Paulista. P.O. Box 467, Presidente Prudente, SP 19060-900, Brazil
[c] Departamento de Química, Faculdade de Filosofia, Ciências e Letras de Ribeirão Preto, Universidade de São Paulo, 14040-901 Ribeirão Preto, SP, Brazil

ARTICLE INFO

Article history:
Received 4 December 2009
Received in revised form
19 July 2010
Accepted 23 August 2010
Available online 26 August 2010

Keywords:
Cerate
Luminescence
Lifetime

ABSTRACT

Luminescent and morphological studies of Sr_2CeO_4 blue phosphor prepared from cerium-doped strontium oxalate precursor are reported. Powder samples were prepared from 5 and 25 mol% Ce^{3+}-doped strontium oxalate as well as from a mechanical mixture of strontium oxalate and cerium oxalate at a 4:1 ratio, respectively. All the samples were characterized by XRD, IR, PLS, and SEM. The luminescent and structural properties of the Sr_2CeO_4 material are little affected by the $SrCO_3$ remaining from precursors. The Sr_2CeO_4 material consists in one-dimensional chains of edge-sharing CeO_6 octahedra that are linked together by Sr^{2+} ions. The carbonate ion might be associated with oxygen ions of the linear chain, and also with the oxygen atoms located in the equatorial position, which consequently affects the charge transfer bands between O^{2-} and Ce^{4+}. As observed by SEM, the morphological changes are related to each kind of precursor and thermal treatment, along with irregular powder particles within the size range 0.5–2 μm.

1. Introduction

Devices based on flat panels, such as field emission displays (FED), are of great interest because of their high image resolution, which is comparable or even superior to those of cathode ray tube (CRT) devices [1]. The search for blue phosphors is of particular importance because of the limited number of stable blue luminescent materials available currently. Danielson et al. [2] have obtained a blue phosphor material from combinatorial chemistry through a solid-state reaction between $SrCO_3$ and CeO_2. This material was analyzed by Rietveld structural refinement, and the luminescent phase was characterized as Sr_2CeO_4 with orthorhombic structure containing one-dimensional chains of edge-sharing CeO_6 octahedra that are linked together by Sr^{2+} ions. This material exhibits excellent luminescent property and maximum emission band around 485 nm, whose intensity changes depending on the employed heat treatment. Some impurity phases such as $SrCO_3$, $SrCeO_3$ and CeO_2 were also detected [3–6].

Some authors [6–9] have assigned the luminescence of the Sr_2CeO_4 material to the charge transfer between Ce^{4+} and O^{2-} because the position and shape of the absorption band, its Stokes shift, and the emission band width (FWHM—full width at half maximum) are characteristic for this type of transition. Some authors have observed that the strong luminescence of Sr_2CeO_4 makes it potentially applicable as blue phosphor material in low pressure mercury vapor lamps [10] and FED [11,12] as well as other types of luminescence devices [13]. Following this observation, several studies about this luminescent material have been conducted, and some synthetic routes have been developed for the preparation of Sr_2CeO_4 powders.

Some authors have observed the effect of temperature and preparation method on particle size. Jiang et al. [11] have observed that the particles increase from 4.0 μm at 1000 °C to 7.5 μm at 1400 °C. The particle shape also became more regular with increase in firing temperature, but at 1400 °C particle coalescence was detected. Through microwave-accelerated hydrothermal (MH) reaction followed by calcinations in air at 1000 °C for 25 h, Khollam et al. [14] have obtained spherical and less coalescent Sr_2CeO_4 particles with an average size of ≈0.5 μm.

The Pechini method [15] has also been used to prepare the Sr_2CeO_4 luminescent blue phosphor in an attempt to decrease the temperature of phase formation [16]. The combustion method [17,18] and a polymer sol–gel route [19,20] involving polyetileglycol (PEG-2000) [21] have also been used.

Based on all these literature reports, it is evident that the methods of preparation as well as the used precursors play an important role in the formation of pure Sr_2CeO_4 luminescent phase. In this sense, our group has previously carried out a

* Corresponding author at: Instituto de Química, UNESP, P.O. Box 355, 14800-970 Araraquara, SP, Brazil. Tel.: +55 16 360 24850; fax: +55 16 3633 2660.
E-mail addresses: jeffersonferrari@gmail.com, ferrari@pg.ffclrp.usp.br (J.L. Ferrari).

0022-2313/$ - see front matter © 2010 Elsevier B.V. All rights reserved.
doi:10.1016/j.jlumin.2010.08.020

systematic study of the thermal decomposition of cerium-doped strontium oxalate with different cerium percentages in order to investigate the different decomposition steps and the influence of the different precursor compositions on the final product [22]. It was demonstrated that cerium-doped (25 mol%) strontium oxalate was the composition that resulted in the best Sr_2CeO_4 luminescent phase formation. Therefore, in this work, a further luminescent and morphological study of the Sr_2CeO_4 phosphor obtained from cerium-doped (25 and 5 mol%) strontium oxalate is reported. A 4:1 mechanical mixture of strontium oxalate and cerium oxalate is also provided in order to allow data comparison as well as a better understanding of the structural and optical properties of the blue phosphor.

2. Experimental procedure

Pure and strontium oxalate and Ce^{3+}-doped and strontium oxalate samples containing Ce^{3+} and 25 mol% were prepared from the mixture of the metal chloride solutions, $SrCl_2 \cdot 6H_2O$ (VETEC, 99% purity) and $CeCl_3 \cdot 7H_2O$ (ALDRICH, 99.999% purity), with a $(NH_4)_2C_2O_4 \cdot H_2O$ (REAGEM, 99% purity) solution. After adjustments to the pH ≈ 4, the temperature was increased to 80 °C and kept at this value under ultrasound stirring for 1 h. The solution was allowed to rest for 4 h, which was followed by filtration and drying of the precipitate under reduced pressure in a desiccator containing silica gel and calcium chloride.

In a separate procedure, cerium oxalate was prepared from a solution of $CeCl_3 \cdot 7H_2O$ (ALDRICH), pH ≈ 1, under stirring and heating with subsequent addition of oxalic acid 3% (drop by drop) (MERCK, PA), followed by addition of a saturated oxalic acid solution, until no precipitation was observed. After filtration, cerium oxalate was dried as described above. The Sr_2CeO_4 material was prepared from heat treatment of cerium-doped strontium oxalate (5 and 25 mol%) precursors as well as from stoichiometric mixtures of strontium oxalate and cerium at a 4:1 ratio, respectively. All precursors were heat treated at 1100 °C, at a heating rate of 20 °C/min, for 12 h, in static air atmosphere.

All products were characterized by X-ray diffractometry (XRD) (SIEMENS D5000 diffractometer, Cu Kα radiation, $\lambda = 1.5418$ Å, graphite monochromator) as well as by infrared spectroscopy (FT-IR) (infrared spectrophotometer Perkin Elmer-Spectrum 2000). Morphology of the oxalate precursor products before and after thermal treatment was analyzed by scanning electron microscopy (SEM) (Zeiss D5M960 microscope). All products displayed blue emission under UV excitation and were investigated by luminescence spectroscopy in the UV–vis region (Fluorolog SPEX F212I fluorescence spectrometer spectrofluorometer equipped with an R928 Hammamatsu photomultiplier and a 450 W Xe lamp). Room temperature kinetic decay measurements were performed by using the same spectrofluorometer equipped with a Xenon pulsed lamp and a phosphorimeter 1934.

3. Results and discussion

All products were analyzed by XRD and the diffractograms are shown in Fig. 1. The X-ray patterns display peaks characteristic of $SrCeO_3$ (PDF 47-1689), $SrCO_3$ (PDF 05-0418), and Sr_2CeO_4 (PDF 22-1422) phases [23], which are shown in Fig. 1. Comparison of relative peak intensities shows that although strontium carbonate is detected in all the samples, Sr_2CeO_4 is the major phase in the samples of 25 mol% cerium-doped strontium oxalate as well as in the samples obtained from the stoichiometric mixture of cerium and strontium oxalates.

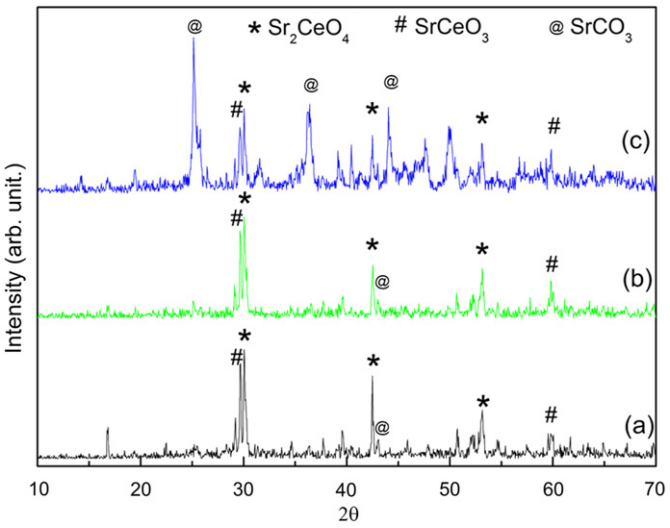

Fig. 1. X-ray diffractograms recorded for the products prepared from the thermal treatment of (a) cerium oxalate and strontium oxalate stoichiometric mixture at a 4:1 ratio, (b) 25 mol% cerium-doped strontium oxalate, and (c) 5 mol% cerium-doped strontium oxalate.

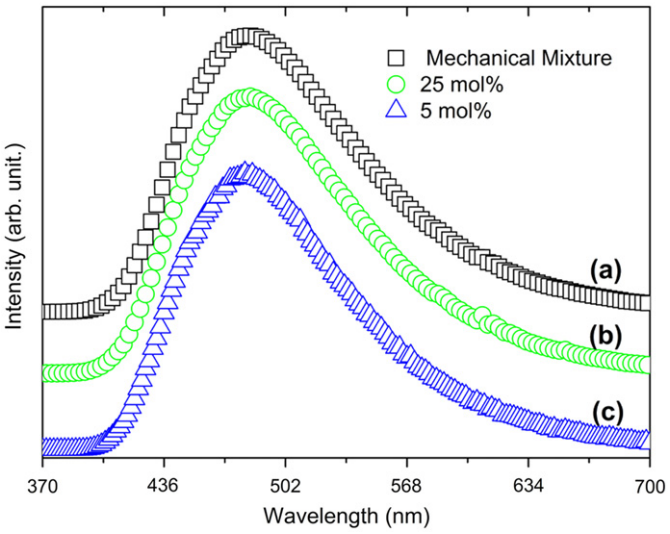

Fig. 2. Emission spectra (λ_{ex}=275 nm) at room temperature recorded for the products prepared from the thermal decomposition of (a) strontium oxalate and cerium oxalate stoichiometric mixture at a 4:1 ratio, (b) 25 mol% cerium-doped strontium oxalate, and (c) 5 mol% cerium-doped strontium oxalate.

Emission spectra (λ_{ex}=275 nm) recorded for the luminescent samples are shown in Fig. 2. One broadband emission in the blue region, centered at 480 nm, can be observed independently of the precursor used. Although not reported and discussed in this work, some preliminary results showed that the material obtained after annealing of stoichiometric mixture of oxalates and Ce^{3+}-doped strontium oxalate depicted a blue emission during the obtainment of the diffractograms. The interaction of the X-ray beam with the sample promoted this effect and made the material a good candidate for use in scintillation. In all cases, the excitation spectra (λ_{em}=480 nm) presented a band at 275 nm with a shoulder around 345 nm. The excitation bands were assigned to the $O^{2-} \rightarrow Ce^{4+}$ charge transfer, as reported by Li et al. [7] for the case of Sr_2CeO_4 prepared by solid-state reaction and sol–gel method.

Fig. 3 shows the deconvoluted excitation spectra, where the most intense band was labeled (1) and the shoulder was designated (2). The values of the corresponding areas related to the observed bands, the ratio between them, and the center of the bands are listed in Table 1.

Considering the edge shared octahedral (CeO_6) structure [2,7], the strong excitation band at 275 nm is assigned to the charge transfer from the axial O^{2-} to the $^2F_{5/2}$ of the Ce^{4+} ions, whereas the shoulder at 340 nm is ascribed to charge transfer from the equatorial O^{2-} to the same energy level of the Ce^{4+} ion. The shoulder at 340 nm in the excitation spectra remained unchanged in all the samples; however, the band around 275 nm was red-shifted. The peak of the weak excitation band located at about 340 nm remained unchanged in all the samples. However, its intensity increased as the strong excitation band red-shifted. In this work, it has been observed that the maximum wavelength of the two bands is present and it is in accordance with the assignment reported by Yongqing et al. [6]. The difference between the areas of bands 1 and 2 decreased for samples with low carbonate quantities present. The carbonate species can contribute to the non-radiative effect. The presence of this species affects directly the excitation intensity and consequently affects the ratio between the areas of bands 1 and 2.

At this point, it is important to remember that the XRD data showed that the sample prepared from 5 mol% cerium-doped strontium oxalate presented strontium carbonate as the main phase, differently from the other two samples (prepared from 25 mol% cerium-doped strontium oxalate and from the 4:1 mechanical mixture), in which Sr_2CeO_4 and $SrCeO_3$ are the main phases.

The decay curves obtained from kinetic decay measurements were monitored under excitation at 275 nm. The best fit adjusted for the exponential curves was first-order type. The generated linear curves as well as the lifetime decay values calculated for

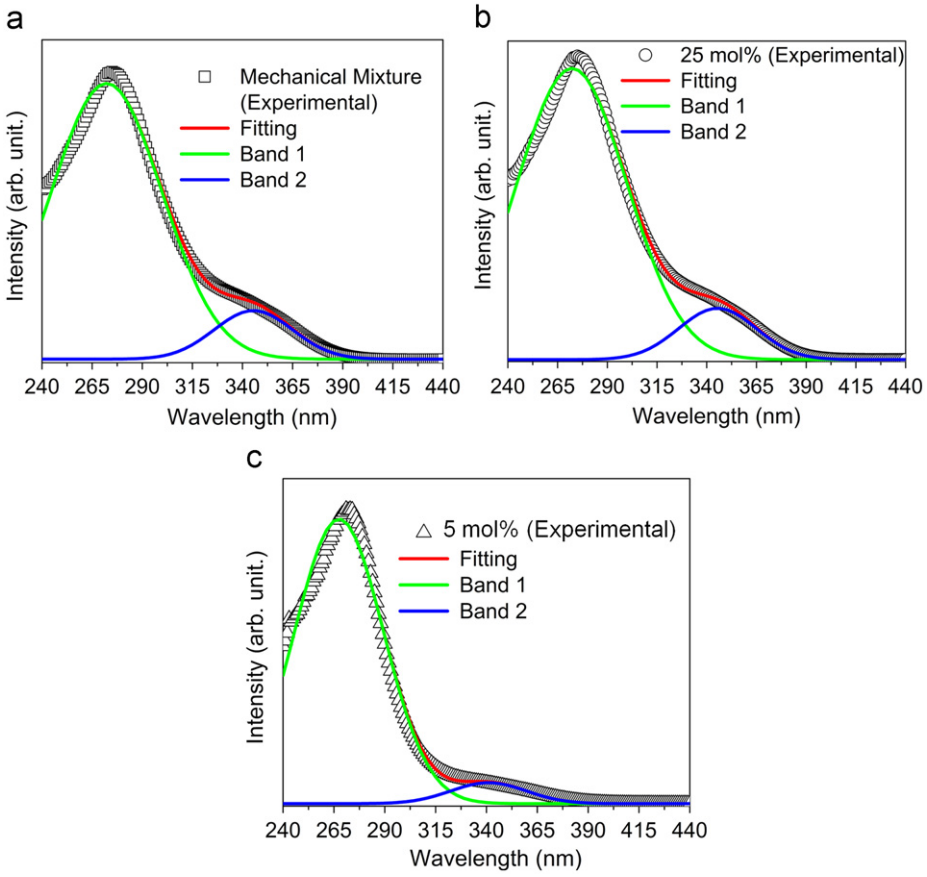

Fig. 3. Deconvolution of the bands observed in the excitation spectra (λ_{em}=480 nm) of the products prepared from the thermal decomposition of (a) strontium oxalate and cerium oxalate stoichiometric mixture at a 4:1 ratio, (b) 25 mol% cerium-doped strontium oxalate, and (c) 5 mol% cerium-doped strontium oxalate.

Table 1
Data calculated from the deconvoluted bands observed in the excitation spectra in Fig. 4, (Band 1 corresponds to energy transfer from axial O^{2-}, Band 2 corresponds to transfer to equatorial).

Samples prepared from thermal treatment	Band	Band center (nm)	Band area	Area (1)/Area (2)
5 mol% cerium-doped strontium oxalate	1	267	6.22×10^{10}	15.87
	2	341	3.92×10^{9}	
25 mol% cerium-doped strontium oxalate	1	272	1.08×10^{11}	8.05
	2	345	1.34×10^{10}	
Strontium oxalate and cerium oxalate stoichiometric mixture at a 4:1 ratio	1	272	1.08×10^{11}	8.06
	2	345	1.34×10^{10}	

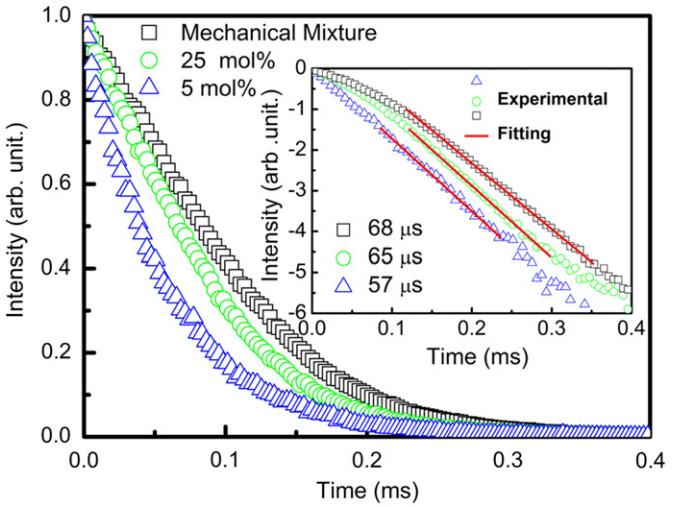

Fig. 4. Photoluminescence emission (λ_{ex}=275 nm) intensity decay curves for the thermal decomposition of strontium oxalate and cerium oxalate stoichiometric mixture at a 4:1 ratio, 25 mol% cerium-doped strontium oxalate and 5 mol% cerium-doped strontium oxalate.

each curve can be viewed in the inset of Fig. 4. The lifetime decay for samples prepared from the oxalate precursor doped with 5 mol% of Ce^{3+} was approximately 57 μs, while the lifetime values for the samples prepared from the oxalate precursor doped with 25 mol% was around 65 μs. As for the sample prepared from the stoichiometric mixture of cerium and strontium oxalates, the lifetime decay was 68 μs. The presence of a larger quantity of strontium carbonate in the samples with shorter lifetime may be attributed to the contribution of the non-radiative process. The sample with longest lifetime is the one that contains a smaller quantity of strontium carbonate.

It is well known that the lifetime (τ) is determined by the radiative decay rate (k_r) and the non-radiative decay rate (k_{nr}), as shown in Eq. (1):

$$\tau = \frac{1}{k_r + k_{nr}} \tag{1}$$

It is also known that the non-radiative decay rate varies significantly in the presence of quenchers. In the present work, strontium carbonate acts as a quencher, being responsible for the shorter lifetime values observed here.

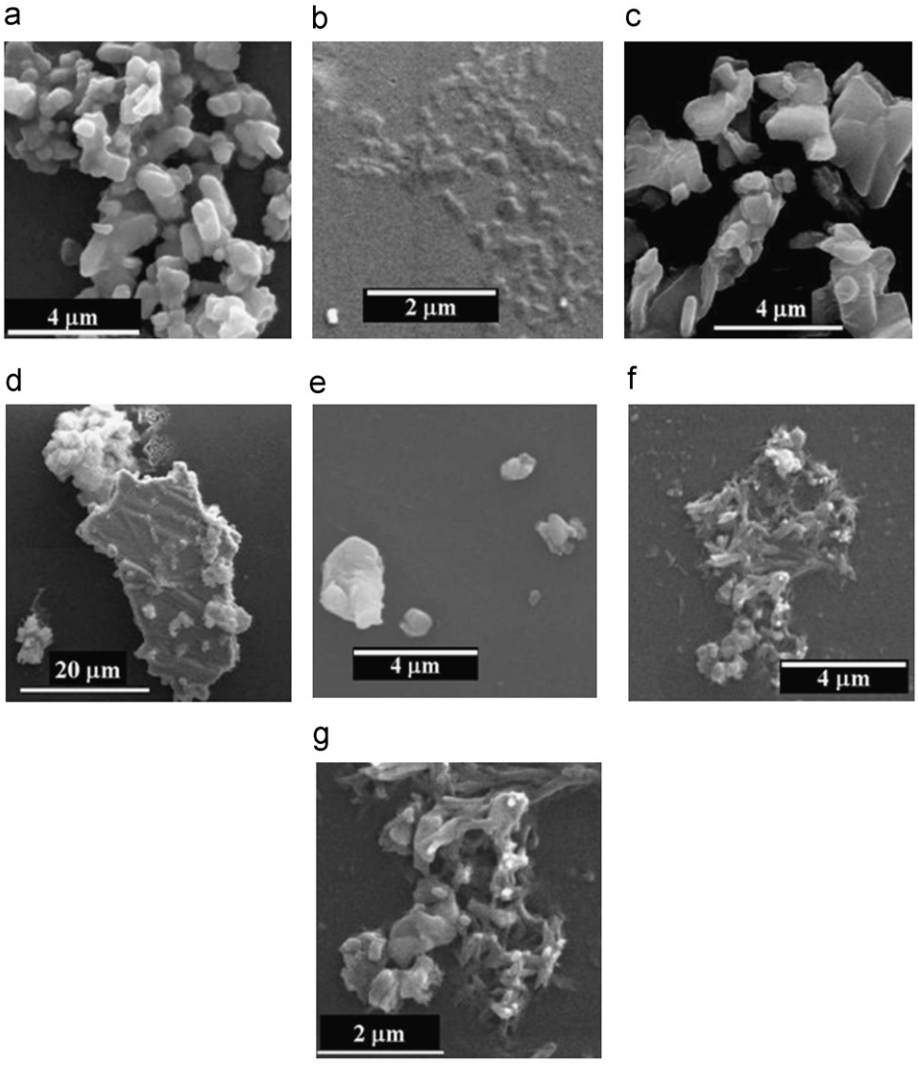

Fig. 5. SEM micrographs of the 5 mol% cerium-doped strontium oxalate samples, (a) before and (b) after thermal treatment; 25 mol% cerium-doped strontium oxalate, (c) before and (d) after thermal treatment; stoichiometric mixture strontium oxalate and cerium oxalate, (e) before and (f, g) after thermal treatment.

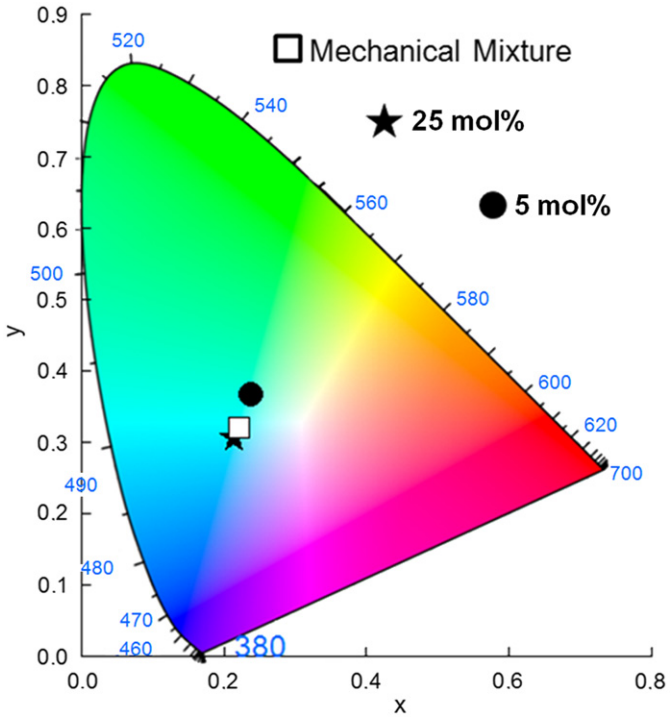

Fig. 6. CIE diagram 1931, and the emission color for each sample.

Fig. 5 presents the SEM results for all the samples, before (a, c, e) and after (b, d, f, g) the thermal treatment. Before the thermal treatment the 5 mol% cerium-doped strontium oxalate precursor, Fig. 5(a), presents the most homogeneous particle shape compared with the other precursor samples. After thermal treatment, Fig. 5(b), particle contraction takes place and the average particle diameter is around 0.5 μm smaller than that obtained by Masui et al. [24] by the co-precipitation technique and solid-state reaction using strontium carbonate and cerium oxide. The 25 mol% cerium-doped strontium oxalate precursor, Fig. 5(c), presents irregular shaped particles, which, after the thermal treatment, Fig. 5(d), form big plates and some agglomerates. Agglomerates are also observed for the sample prepared from the stoichiometric mixture, Fig. 5(e), mainly after the thermal treatment, Fig. 5(f) and (g), with the presence of lengthened particles. In all the cases, realization of the thermal treatment leads to particle contraction and an initial sintering process.

Based on the emission spectra, it was possible to see the color of the emission of each sample in the CIE diagrams 1931. Fig. 6 shows the CIE diagram 1931, and the color of each sample is directly dependent on the presence of the carbonate species.

4. Conclusions

XRD results showed that the 5 mol% cerium-doped strontium oxalate sample is formed by a mixture of Sr_2CeO_4, $SrCeO_3$ and $SrCO_3$ phases, the latter phase being the major one. The blue phosphors prepared from 25 mol% cerium-doped strontium oxalate and from the stoichiometric mixture proved to contain the best composition for preparing the Sr_2CeO_4 luminescent phase with attractive luminescent property, although $SrCeO_3$ and $SrCO_3$ are still detected. The sample obtained from mechanical mixture between the oxalates resulted in much longer decay lifetime, compared with other samples and also with other works published in the literature, making the material a potential candidate for optical applications. The emission observed when these materials were excited by X-ray radiation shows that they are also applicable as scintillator for capturing images.

Acknowledgements

The authors thank FAPESP and CNPq for the financial support. J.L. Ferrari thanks FAPESP for the scholarship (JLF).

References

[1] M. Leskelä, J. Alloys Compd. 275 (1998) 702.
[2] E. Danielson, M. Devenney, D.M. Gianquita, J.H. Golden, R.C. Haushalter, E.W. McFarland, D.M. Poojary*, C.M. Reaves, W.H. Weinberg, X.D. Wu, J. Mol. Struct. 470 (1998) 229.
[3] S.K. Shi, J.M. Li, J.Y. Wang, R.F. Wang, J. Zhou., J. Rare Earths 22 (2004) 833.
[4] C.H. Lu, C.T. Chen, J. Sol–Gel Sci. Technol. 43 (2007) 179.
[5] S.L. Fu, J. Dai, Q.K. Ding, J. Inorg. Mater. 21 (2006) 357.
[6] Z. Yongqing, Z. Xueling, Y. Guozhong, M. Yuan, Y. Sumei, G. Zaihong, J. Rare Earths 24 (2006) 281.
[7] L. Li, S. Zhou, S. Zhang, Chem. Phys. Lett. 453 (2008) 283.
[8] P.N. Yocom, Electrochem. Soc. Interface 3 (1994) 26.
[9] X. Yu, X.H. He, S.P. Yang, X. Yang, X. Xu, Mater. Lett. 58 (2003) 48.
[10] R. Sankar, G.V.Subba Rao, J. Electrochem. Soc. 147 (2000) 2773.
[11] Y.D. Jiang, F. Zhang, C.J. Summers., Appl. Phys. Lett. 74 (1999) 1677.
[12] X. Liu, Y. Luo, J. Lin, J. Cryst. Growth 290 (2006) 266.
[13] Van L. Pieterson, S. Soverna, A. Meijerink, J. Electrochem. Soc. 147 (2000) 4688.
[14] Y.B. Khollam, S.B. Deshpande, P.K. Khanna, P.A. Joy, H.S. Potdar, Mater. Lett. 58 (2004) 2521.
[15] M.P. Pechini, (USA), Method of preparing lead and alkaline earth titanates and niobates and coating method using the same to form a capacitor, US Patent no. 3330697, 1963.
[16] O.A. Serra, V.P. Severino, P.S. Calefi, S.A. Cicillini, J. Alloys Compd. 323 (2001) 667.
[17] J. Gomes, A.M. Pires, O.A. Serra, Quim. Nova 21 (2004) 706.
[18] J. Gomes, O.A. Serra, A.M. Pires, Ecl. Quím 27 (2002) 187 (special issue).
[19] R. Ghildiyal, P. Page, K.V.R. Murthy, J. Lumin. 124 (2007) 217.
[20] X. Desong, G. MengLian, Q. Xueqing, Y. Dongjie, C. KokWai, J. Rare Earths 24 (2006) 289.
[21] S.J. Chen, Z. Yu, J.M. Hong, Z. Xue, X.Z. You, Solid State Commun. 130 (2004) 281.
[22] J.L. Ferrari, A.M. Pires, C.A. Ribeiro, M.R. Davolos, Ecl. Quím. 27 (2002) 315 (special issue).
[23] Powder Diffraction File PDF-2 data base sets 1-44, Pensylvannia Joint Committee on Powder Diffraction Standards–International Center for Diffraction Data, 1988, PDG number 43-1014 (CD-ROM).
[24] T. Masui, T. Chiga, N. Iamanaka, G. Adashi, Mater. Res. Bull. 38 (2003) 17.